

Pseudospectra of Matrix Polynomials that are Expressed in Alternative Bases

Robert M. Corless, Nargol Rezvani and Amirhossein Amiraslani

Mathematics Subject Classification (2000). Primary 15A42; Secondary 41A05.

Keywords. Pseudospectra, matrix polynomial, conditioning, Lebesgue functions, Lebesgue constants.

Abstract. Spectra and pseudospectra of matrix polynomials are of interest in geometric intersection problems, vibration problems, and analysis of dynamical systems. In this note we consider the effect of the choice of polynomial basis on the pseudospectrum and on the conditioning of the spectrum of regular matrix polynomials. In particular, we consider the direct use of the Lagrange basis on distinct interpolation nodes, and give a geometric characterization of “good” nodes. We also give some tools for computation of roots at infinity via a new, natural, reversal. The principal achievement of the paper is to connect pseudospectra to the well-established theory of Lebesgue functions and Lebesgue constants, by separating the influence of the scalar basis from the natural scale of the matrix polynomial, which allows many results from interpolation theory to be applied.

1. Introduction

A *matrix polynomial* $\mathbf{P}(z)$ is a matrix with entries polynomial in the variable z ; isomorphically, $\mathbf{P}(z)$ is a polynomial in z with matrix coefficients. We will use s for the dimension of the matrix, and n for the degree of the polynomial. In this paper, we consider only *regular* matrix polynomials, that is, those with determinant not identically zero.

Matrix polynomials find many applications: see, for example, [11]. Geometric intersection problems are studied using matrix polynomials in [17], and applications using the Lagrange basis in [7].

This work was partially funded by the Natural Sciences and Engineering Research Council of Canada, and by the MITACS Network of Centres of Excellence.

The spectrum of a matrix polynomial $\mathbf{P}(z)$ is the set of values $\lambda \in \mathbf{C}$ such that $\mathbf{P}(\lambda)$ is *singular*. These values are called *polynomial eigenvalues* or *latent roots* or, more simply, *eigenvalues*. They simultaneously generalize both roots of polynomials and eigenvalues of matrices. *Pseudospectra* of matrix polynomials are polynomial eigenvalues of perturbed or noisy matrix polynomials. Wherever polynomial eigenvalues are useful, pseudospectra are (generally speaking) also useful, and sometimes more so.

In [1] a lemma is given, analogous to an important lemma of [21], which separates out the contributions to the pseudospectra from the polynomial basis used. Therefore, using this lemma, one may try to understand the influence of the geometry of the interpolation nodes on the pseudospectra. We reproduce this lemma and its proof below, as Proposition 2.1.

Other papers have examined the influence of the placement of the nodes on the conditioning of polynomial roots [6][8], and there has been considerable work on the influence of the choice of basis itself on the conditioning of polynomial roots; see, for example, the references of the paper [8].

1.1. Definitions

In some of what follows, we could use a general field \mathbb{K} instead of \mathbf{C} , the field of complex numbers. However, in this paper, we will restrict ourselves to \mathbf{C} , with the understanding that floating-point computation (possibly arbitrary precision) will be used as necessary. Unless otherwise specified, we use the vector 2-norm (Euclidean norm) and the subordinate matrix norm $\|\mathbf{A}\|$, which is equal to the largest singular value of \mathbf{A} .

- The set $\mathbf{C}[z]$ is the set of all polynomials of degree at most n with coefficients from \mathbf{C} . Alternatively, it is the set of \mathbf{C} -linear combinations of polynomial *basis functions* $\phi_k(z)$, $0 \leq k \leq n$. Typically one takes $\phi_k(z) = z^k$, but we shall consider other choices in this paper.
- An $s \times s$ *matrix polynomial* $\mathbf{P}(z)$ of degree n is an element of $\mathbf{C}[z]^{s \times s}$. Typically we will say that the true or actual degree of $\mathbf{P}(z)$ is the maximum degree of the entries of $\mathbf{P}(z)$, which we will take to be n , but in the cases of practical interest here (Lagrange basis and Bernstein basis) the degree is not always immediately evident; in that case, n will be an upper bound on the true degree.
- Given $\mathbf{P}(z) = \sum_{k=0}^n \mathbf{C}_k \phi_k(z)$, with $\mathbf{C}_k \in \mathbf{C}^{s \times s}$, then the matrices \mathbf{C}_k are called the coefficients of $\mathbf{P}(z)$ in the basis ϕ .
- The set of *polynomial eigenvalues* of $\mathbf{P}(z)$ is defined to be

$$\sigma(\mathbf{P}) = \{\lambda \in \mathbf{C} : \det \mathbf{P}(\lambda) = 0\}. \quad (1.1)$$

- The weighted ε -*pseudospectrum* of $\mathbf{P}(z)$ is defined to be

$$\Lambda_\varepsilon(\mathbf{P}) = \{\lambda \in \mathbf{C} : \det(\mathbf{P} + \Delta\mathbf{P})(\lambda) = 0, \|\Delta\mathbf{C}_k\| \leq \varepsilon \alpha_k, k = 0, \dots, n\} \quad (1.2)$$

where $\alpha_k \geq 0$ are the (given) weights, not all zero, and

$$\Delta \mathbf{P}(z) = \sum_{k=0}^n \Delta \mathbf{C}_k \phi_k(z). \quad (1.3)$$

- **Barycentric Form:** (See [4, 13]) Let $\mathbf{P}(z)$ be the matrix polynomial taking on the values $[\mathbf{P}_0, \mathbf{P}_1, \dots, \mathbf{P}_n]$ at the distinct nodes $\mathbf{x} = [x_0, x_1, \dots, x_n]$. In the Lagrange basis, $\mathbf{P}(z)$ can be represented in the *barycentric form* [4]

$$\mathbf{P}(z) = \ell(z) \sum_{k=0}^n \frac{w_k \mathbf{P}_k}{(z - x_k)}, \quad (1.4)$$

where

$$\ell(z) = (z - x_0)(z - x_1) \dots (z - x_n) \quad (1.5)$$

and the barycentric weights are, for $0 \leq k \leq n$,

$$w_k = \prod_{j \neq k} \frac{1}{(x_k - x_j)}. \quad (1.6)$$

This form is numerically stable to evaluate (in [13] it is shown that the numerical evaluation of a scalar polynomial is stable in this form; the generalization to matrix polynomials is immediate). Note that if $\phi_k(z) = L_k(z) := w_k \ell(z)/(z - x_k)$, then the values \mathbf{P}_k are the coefficients of the polynomial in this basis.

2. The influence of the polynomial basis

We begin with a proposition that allows us to separate the influence of the basis from the influence of the matrix polynomial.

Proposition 2.1. [1][21] *Given weights $\alpha_k \geq 0$, and a basis $\phi_k(z)$, define*

$$B(\lambda) = \sum_{k=0}^n \alpha_k |\phi_k(\lambda)|. \quad (2.1)$$

Then the pseudospectrum of $\mathbf{P}(z)$ may be alternatively characterized as

$$\Lambda_\varepsilon(\mathbf{P}) = \{\lambda \in \mathbb{C} : \|\mathbf{P}^{-1}(\lambda)\| \geq (\varepsilon B(\lambda))^{-1}\}. \quad (2.2)$$

Proof. This proof is taken from [1], and was there modelled exactly on the one for the monomial basis in [21]. Let

$$\mathcal{S} = \{\lambda \in \mathbb{C} : \|\mathbf{P}^{-1}(\lambda)\| \geq (\varepsilon B(\lambda))^{-1}\} \quad (2.3)$$

We show that this set is equal to $\Lambda_\varepsilon(\mathbf{P})$.

First, take $\lambda \in \Lambda_\varepsilon(\mathbf{P})$. We show that $\lambda \in \mathcal{S}$.

- If λ is an eigenvalue of $\mathbf{P}(z)$, then by convention $\|\mathbf{P}^{-1}(\lambda)\| = \infty$ and so $\lambda \in \mathcal{S}$.

- If λ is not an eigenvalue of $\mathbf{P}(z)$ then $\mathbf{P}(\lambda)$ is nonsingular. Since $\mathbf{P}(\lambda) + \Delta\mathbf{P}(\lambda) = \mathbf{P}(\lambda) (\mathbf{I} + \mathbf{P}^{-1}(\lambda)\Delta\mathbf{P}(\lambda))$ is singular, $\|\mathbf{P}^{-1}(\lambda)\Delta\mathbf{P}(\lambda)\| \geq 1$ must hold and so:

$$\begin{aligned} 1 &\leq \|\mathbf{P}^{-1}(\lambda)\| \left(\sum_{k=0}^n \|\Delta\mathbf{C}_k\| |\phi_k(\lambda)| \right) \\ &\leq \|\mathbf{P}^{-1}(\lambda)\| \left(\sum_{k=0}^n \varepsilon \alpha_k |\phi_k(\lambda)| \right) \\ &\leq \|\mathbf{P}^{-1}(\lambda)\| \varepsilon B(\lambda) \end{aligned}$$

and so $\lambda \in \mathcal{S}$.

Now let $\lambda \in \mathcal{S}$ and assume $\mathbf{P}(\lambda)$ is nonsingular.

1. Choose a unit vector \mathbf{y} such that $\|\mathbf{P}^{-1}(\lambda)\mathbf{y}\| = \|\mathbf{P}^{-1}(\lambda)\|$.

2. Consider the vector $\mathbf{u} = \frac{\mathbf{P}^{-1}(\lambda)\mathbf{y}}{\|\mathbf{P}^{-1}(\lambda)\|}$, which is also a unit vector.

Then (see [12]) there exists a matrix \mathbf{H} with $\|\mathbf{H}\| = 1$ and $\mathbf{H}\mathbf{u} = \mathbf{y}$. Now define \mathbf{E} to be $\mathbf{E} = -\mathbf{H}\|\mathbf{P}^{-1}(\lambda)\|$. Then

$$(\mathbf{P}(\lambda) + \mathbf{E})\mathbf{u} = \frac{\mathbf{y}}{\|\mathbf{P}^{-1}(\lambda)\|} - \frac{\mathbf{y}}{\|\mathbf{P}^{-1}(\lambda)\|} = 0 \quad \text{and} \quad \|\mathbf{E}\| = \frac{1}{\|\mathbf{P}^{-1}(\lambda)\|} \leq \varepsilon B(\lambda). \quad (2.4)$$

Define (where $\text{sign}(z) = z/|z|$ if $z \neq 0$, and 0 otherwise)

$$\Delta\mathbf{C}_k = \text{sign}(\overline{\phi_k(\lambda)}) \alpha_k B^{-1}(\lambda) \mathbf{E}.$$

So

$$\begin{aligned} \Delta\mathbf{P}(\lambda) &= \sum_{k=0}^n \Delta\mathbf{C}_k \phi_k(\lambda) \\ &= \sum_{k=0}^n \text{sign}(\overline{\phi_k(\lambda)}) \phi_k(\lambda) \alpha_k B^{-1}(\lambda) \mathbf{E} \\ &= \sum_{k=0}^n |\phi_k(\lambda)| \alpha_k B^{-1}(\lambda) \mathbf{E} \\ &= B(\lambda) B^{-1}(\lambda) \mathbf{E} = \mathbf{E} \end{aligned}$$

and

$$\|\Delta\mathbf{C}_k\| \leq \alpha_k \varepsilon \implies \lambda \in \Lambda_\varepsilon(\mathbf{P}). \quad (2.5)$$

—‡

Remarks. This proposition allows us to separate some of the properties of the polynomial $\mathbf{P}(z)$ from the properties of the basis. In particular, notice that the left-hand side of the inequality in this characterization of the pseudospectrum is *basis-independent*, being merely a property of the size of $\mathbf{P}(\lambda)$, whereas the right-hand side of the inequality depends only on the tolerance ε and the value of

the scalar function $B(z)$ at $z = \lambda$, which depends only on the basis and on the weights α_k .

When all $\alpha_k = 1$, the function $B(z)$, in the case of Lagrange interpolation, is precisely what is known as the *Lebesgue function* of the set of interpolation nodes [19]. There is an extensive theory of such functions, and their connection to the problem of conditioning. In the standard notation, for $\alpha_k \equiv 1$, $B(z) = \lambda_n(\mathbf{x}; z)$.

This characterization will allow the fast continuation techniques of [16] to be used to compute the pseudospectra efficiently. We do not do this here, because our interest is in working with a fixed matrix polynomial and then changing the basis; for this purpose, a high-resolution computation of $\|\mathbf{P}^{-1}(z)\|$ (on many grid points in z), by means of a singular value computation for each grid point, followed by a simpler scalar computation of (possibly several different) $B(z)$ on the same grid then allows standard contouring software to be used. In this paper, we used Maple and Matlab to generate the figures. We plan in future work to adapt and implement the techniques of [16] for faster computation of pseudospectra in a given fixed basis.

3. Reversing Polynomials expressed in a Lagrange Basis

When working with matrix polynomials, it is standard to use a *strong linearization* to convert the polynomial eigenvalue problem to a generalized eigenvalue problem [3, 14, 15]. A strong linearization, as opposed to weaker linearizations, preserves eigenstructure at infinity as well as the finite eigenstructure. This is usually studied through the reversal $\mathbf{P}^*(z) = z^n \mathbf{P}(1/z)$ which maps $z = 0$ to ∞ and vice versa. If the matrix polynomial $\mathbf{P}(z)$ is expressed in the monomial basis, then $z = 0$ is already a distinguished point, but in the Lagrange case we are considering here, $z = 0$ may be outside the domain of interest; for example, it may be far from all the nodes, and thus not well-represented numerically. It turns out that we may reverse a matrix polynomial $\mathbf{P}(z)$ expressed in a Lagrange basis directly, without making $z = 0$ a special point, by choosing another point $z = x_c$, which may be more relevant to the geometry of the nodes we are using.

Let $\mathbf{P}(z)$ be the matrix polynomial taking on the values $[\mathbf{P}_0, \mathbf{P}_1, \dots, \mathbf{P}_n]$ at the distinct nodes $\mathbf{x} = [x_0, x_1, \dots, x_n]$.

The geometry of these nodes may suggest a natural centre x_c and a natural radius R . The radius R and centre x_c are meant to roughly cover the nodes with a circle of radius R centred at x_c . Here we take as parameters R and the nominal centre x_c , which must be different from any node (because the centre will be sent to infinity by the reversal process). That is, one must choose $x_c \neq x_k$ for any $0 \leq k \leq n$, and, moreover, for numerical stability reasons we should also ensure that x_c is not too close to any node, either.

To be precise, one would often like to choose $x_c = (x_0 + x_1 + \dots + x_n)/(n+1)$ as the arithmetic mean of the nodes, and choose

$$R = (|x_0 - x_c| \cdot |x_1 - x_c| \cdots |x_n - x_c|)^{1/(n+1)}$$

as the geometric mean of the distances to the centre. However, it may happen (e.g. for $\mathbf{x} = [-1, 0, 1]$) that the arithmetic mean of the nodes is itself a node, and because the centre will be sent to infinity by the reversal process, we will have to adjust. In this small example it may suffice to choose instead $x_c = 1/10$, or perhaps $x_c = i/10$, near to the arithmetic mean of the nodes, but not too near.

In the Lagrange basis, $\mathbf{P}(z)$ can be stably represented as in equations (1.4–1.6). That is, we use the basis (for fixed set of distinct nodes)

$$\phi_k(z) = \frac{w_k \ell(z)}{z - x_k} \quad (3.1)$$

from now on in this paper, unless otherwise specified. Note that $\phi_k(x_j) = \delta_j^k$ is 1 when $k = j$ and 0 otherwise; and note that $\phi_k(z)$ is indeed a polynomial in z , of degree n .

In what follows we denote dual quantities (reversed nodes, etc) with a superscript $*$. This is not a complex conjugate. Given a new nominal centre x_c^* and a new typical radius R^* , define the reverse nodes x_k^* as follows,

$$x_k^* = x_c^* + \frac{RR^*}{x_k - x_c}. \quad (3.2)$$

Note that x_c^* is automatically different from any reversed node x_k^* . In fact, we usually choose $x_c^* = 0$ and $R^* = 1$.

These nodes allow us to define a ‘reversed’ $\ell^*(z)$ and ‘reversed’ barycentric weights w_k^* as

$$\ell^*(z) = (z - x_0^*)(z - x_1^*) \cdots (z - x_n^*) \quad (3.3)$$

and

$$w_k^* = \prod_{j \neq k} \frac{1}{(x_k^* - x_j^*)}. \quad (3.4)$$

Reversing the reversed nodes gets us back where we started: Equation (3.2) gives

$$x_k = x_c + \frac{RR^*}{x_k^* - x_c^*}. \quad (3.5)$$

Definition 3.1. The reversal of $\mathbf{P}(z)$ is

$$\mathbf{P}^*(z) = (z - x_c^*)^n \mathbf{P}\left(x_c + \frac{RR^*}{z - x_c^*}\right). \quad (3.6)$$

Proposition 3.2. For $k = 0 \dots n$, the values of $\mathbf{P}^*(z)$ at the reversed nodes $z = x_k^*$ are, for $k = 0, 1, \dots, n$,

$$\mathbf{P}_k^* = \mathbf{P}^*(x_k^*) = \frac{(RR^*)^n}{(x_k - x_c)^n} \mathbf{P}_k. \quad (3.7)$$

Proof.

$$\begin{aligned}
\mathbf{P}^*(z) &= (z - x_c^*)^n \mathbf{P}\left(x_c + \frac{RR^*}{z - x_c^*}\right) \\
&= (z - x_c^*)^{n+1} \prod_{j=0}^n \left(x_c + \frac{RR^*}{z - x_c^*} - x_j\right) \sum_{k=0}^n \frac{w_k \mathbf{P}_k}{(x_c - x_k)(z - x_c^*) + RR^*} \\
&= \prod_{j=0}^n \left((x_c - x_j)(z - x_c^*) + RR^*\right) \sum_{k=0}^n \frac{w_k \mathbf{P}_k / (x_c - x_k)}{\left(z - x_c^* + \frac{RR^*}{x_c - x_k}\right)} \\
&= \prod_{j=0}^n (x_c - x_j) \prod_{j=0}^n \left(\left(z - x_c^*\right) + \frac{RR^*}{x_c - x_j}\right) \sum_{k=0}^n \frac{w_k \mathbf{P}_k / (x_c - x_k)}{(z - x_k^*)} \\
&= \prod_{j=0}^n (z - x_j^*) \sum_{k=0}^n \left(\frac{w_k \mathbf{P}_k}{(z - x_k^*)} \prod_{j=0, j \neq k}^n (x_c - x_j)\right)
\end{aligned}$$

Comparing equation (3.12) with the above, we get

$$w_k^* \mathbf{P}_k^* = w_k \mathbf{P}_k \prod_{j=0, j \neq k}^n (x_c - x_j) \quad (3.8)$$

for $0 \leq k \leq n$. Considering Equations (3.2) and (3.4) we find

$$\begin{aligned}
w_k^* &= \prod_{j=0, j \neq k}^n \frac{(x_k - x_c)(x_j - x_c)}{RR^*(x_j - x_k)} \\
&= \frac{(x_k - x_c)^n}{(RR^*)^n} \prod_{j=0, j \neq k}^n (x_c - x_j) \prod_{j=0, j \neq k}^n \frac{1}{(x_k - x_j)} \\
&= \frac{(x_k - x_c)^n}{(RR^*)^n} \prod_{j=0, j \neq k}^n (x_c - x_j) w_k.
\end{aligned}$$

Using the equality in equation (3.8) we find

$$\frac{(x_k - x_c)^n}{(RR^*)^n} \prod_{j=0, j \neq k}^n (x_c - x_j) w_k \mathbf{P}_k^* = w_k \mathbf{P}_k \prod_{j=0, j \neq k}^n (x_c - x_j) \quad (3.9)$$

Hence we have the (apparently numerically stable if x_c is not too close to any x_k) formula

$$\mathbf{P}_k^* = \frac{(RR^*)^n}{(x_k - x_c)^n} \mathbf{P}_k, \quad (3.10)$$

or, equivalently,

$$\mathbf{P}_k^* = (x_k^* - x_c^*)^n \mathbf{P}_k. \quad (3.11)$$

—□

Remarks. If the coefficient of z^n in the monomial basis expansion of $\mathbf{P}(z)$, namely $\sum_{k=0}^n w_k \mathbf{P}_k$, is singular, then $\mathbf{P}^*(z)$ will have (possibly multiple) eigenvalues at $z = x_c^*$, and vice-versa. Thus, reversal allows the study of eigenvalues at infinity in the original case by studying finite eigenvalues at $z = x_c^*$. Note also that in the new Lagrange basis represented by the reversed nodes and values, $\mathbf{P}^*(z)$ can be stably represented as

$$\mathbf{P}^*(z) = \ell^*(z) \sum_{k=0}^n \frac{w_k^* \mathbf{P}_k^*}{(z - x_k^*)}. \quad (3.12)$$

4. Pseudospectra and Conditioning

The backward error and conditioning of polynomial eigenvalue problems expressed in the monomial basis is studied in [20]. Backward error and conditioning for scalar polynomials expressed in other bases are studied in many places, for example in [8]. Pseudospectra and conditioning are connected, in that in the limit as $\varepsilon \rightarrow 0$ the pseudospectra degenerate to small circles of radius $K(\lambda)\varepsilon + o(\varepsilon)$, where $K(\lambda)$ is the condition number of λ . In the scalar case $s = 1$, we can see that the influence of the basis on the condition number is to explicitly replace $K(\lambda)$ by $B(\lambda)\hat{K}$. That is, a small $B(\lambda)$ improves the conditioning.

Considering pseudospectra of matrix polynomials, in the case $s > 1$, Proposition 2.1 shows that it is still true that if $B(\lambda)$ is small, then it is as if ε was smaller—that is, the λ satisfying the inequality will be required to be closer to the polynomial eigenvalues. Thus we see that $B(\lambda)$ being small makes pseudospectra closer to spectra. In the pseudospectral computation, we can also make the computation relative to the size of the coefficients, if we take $\alpha_k = \|\mathbf{C}_k\|$. In that case, $B(\lambda)$ is still scalar, but no longer independent from the polynomial; we believe that this may be a useful process. In the examples of this paper, we choose only $\alpha_k = 1$, and try to arrange that all the \mathbf{C}_k are $O(1)$.

These observations motivate the question, where is $B(z)$ small? A related question that occurs in standard interpolation problems where we may choose the nodes is: What placement of nodes is good, or optimal, for finding polynomial eigenvalues in a given region? Note that in our case we are really concerned with the first problem: Given a fixed set of nodes, for what region is $B(z)$ small, where we can expect reasonable accuracy?

One key observation is that both these questions, the choice of node placement *and* the question of how big the ‘good’ region is for a given set of nodes, become *scalar problems*. This is both an advantage (for understanding) and a disadvantage, in that if s is large, then we have to control the conditioning at ns eigenvalues by placing only $n + 1$ nodes. However, the influence of the nodes can be understood without consideration of the actual eigenvalues.

If we take all $\alpha_k = 1$, then we may profit from well-known results on Lebesgue functions and their maxima on subsets of \mathbb{C} , known as *Lebesgue constants* [19]. As

a referee has pointed out, there is also a connection with so-called *Fekete points* and *transfinite diameter* or *transfinite capacity*, which we take up in a later section.

4.1. Geometric Interpretation

We see that

$$B(z) = \sum_{k=0}^n \alpha_k \prod_{j \neq k} \frac{|z - x_j|}{|x_k - x_j|} \quad (4.1)$$

(using the definition of w_k). Each term in this sum can be interpreted as a hypervolume. In the case of 3 points, for example, each term is simply an area, the area of a rectangle with sides $|z - x_0|/|x_2 - x_0|$ and $|z - x_1|/|x_2 - x_1|$, for example. Thus the influence of the geometry of the nodes can be interpreted in terms of hypervolumes of hyperboxes with side lengths given by the distances to all but one node; and we then add over all nodes. Any point z such that these lengths are all less than 1 is in a good state—each hypervolume will be less than 1, then, and the sum less than $(n + 1)$. At each node, of course, all terms but one are 0, and the remaining one is 1. It is clear that $B(z) \geq 1$ for all z , in fact.

Let us consider the case of just two real nodes (and $\alpha_k = 1$). In this case

$$B(z) = \frac{|z - x_0|}{|x_1 - x_0|} + \frac{|z - x_1|}{|x_0 - x_1|}, \quad (4.2)$$

which (for example by graphing, or by inequality arguments) we see is constant and minimal everywhere on the interval $x_0 \leq z \leq x_1$. One can see that the contours of $B(z)$ in the complex plane are ellipses, with foci at x_0 and x_1 .

Indeed, this two-node case gives an instance of a classical problem, *Fermat's problem* (sometimes called Steiner's problem) from plane geometry [18]. The problem there is to find a point in a triangle such that the (weighted) sum of the lengths is minimal. That corresponds to finding the place where $B(z)$ is minimal. Then, by the fact that functions are usually flat near their minima, we would find a good region near that minimal point for zero-finding. In the two-node case above, this degenerates, and the constant minimum occurs anywhere on a line segment joining the two nodes, since the barycentric weights are equal.

The Fermat problem analogy becomes more remote, with more nodes: instead of trying to minimize the sum of the lengths, we are trying to minimize the sum of the areas (in case of three nodes) or volumes (in case of four nodes) or hypervolumes (for more than four nodes).

However, in the case of three nodes forming the vertices of an equilateral triangle, at roots of unity¹, we have minimality at the centre, where again $B(z) = 1$. See Figure 1. In Figure 2 we see the same construction with four nodes arranged in a square (at 1, i , -1 , and $-i$). Again we see small values of $B(z)$ in the interior of the region defined by the nodes, with rapid growth outside. Similarly, in Figures 3

¹With nodes at the roots of unity, the barycentric weights have a particularly simple form: $w_k = 1/\ell'(x_k) = x_k/n$. These have equal moduli, making $B(z) = |z^n - 1| \sum_{k=0}^{n-1} 1/(n|z - x_k|)$ relatively easy to minimize.

and 4 we see the same construction with five nodes and eight nodes, respectively, at roots of unity.

Outside the geometric figure formed by the small contours—like a rounded triangle with inward-curved sides in the 3-node case—we see contours roughly equally spaced. However, the values of the k th contour is $r^{k^2/4}$, which was chosen for good spacing for small k ; this grows faster than geometrically, ultimately, but that is not completely relevant here. The growth of $B(z)$ outside the enclosure of the nodes is indeed fast, ultimately $O(\rho^n)$ where $\rho = |z|$, as $\rho \rightarrow \infty$. This means that *large polynomial eigenvalues* have their pseudospectra spread by a factor ρ^n , where ρ is the distance to the interpolation nodes.

It is natural to be curious about the maximum $B(z)$ inside the n -gon enclosed by the figure, which is the Lebesgue constant for the interpolation points. The contour at that height crosses itself, showing the loops in the figures. By brute computation, we find that, for n up to 100, this maximum value grows slowly, up to about 1.75, and indeed appears to settle down to logarithmic growth. This agrees with the classical result that the Lebesgue constant for any set of nodes must grow at least as fast as $2/\pi \ln n$ [19]. This slow growth is to be contrasted with the behaviour of $B(z)$ for the *monomial* basis, which is also known to be good for evaluation and rootfinding on the unit disk. It is easily seen that in this case (for $\alpha_k = 1$) that $B(z) = 1 + |z| + |z|^2 + \dots + |z|^{n-1}$, or $(|z|^n - 1)/(|z| - 1)$, which approaches n at the edge of the disk. We see that interpolation at roots of unity provides an improvement, of a factor of $O(\log(n)/n)$, for the maximum “spreading” of pseudospectra inside the unit disk.

Geometric Characterization of good nodes: these observations tell us that optimal node placement has geometrically regular spacing, as well as being close to the spectrum. If any of the hyperboxes are very much ‘skinnier’ than the others, then the volumes will vary widely, and $B(z)$ will fail to have its $n + 1$ terms be of roughly equal size; by the equidistribution principle, then, $B(z)$ will not be as small as it could be.

As stated before, if z is such that its distance to each node is less than the distance of the nodes to each other, then each side of the hyperbox will be less than 1, and the volumes will be less than 1. This characterization of closeness also encourages regularity of the nodes.

4.1.1. Lebesgue points, Fekete points and transfinite diameter. The problem of deciding when a polynomial is of small maximum norm on a given compact set $\Omega \subset \mathbb{C}$ is an old one, because this is important for interpolation problems. Provided that Ω has at least $n + 1$ points in it, then there is a unique polynomial of degree n called the Chebyshev polynomial of Ω and written $T_n(z, \Omega)$ which has minimal (over all monic polynomials) maximum norm on Ω [19]. Let $\|T_n(z, \Omega)\|_\infty = m_n$ be this minimal maximum norm. If there are infinitely many points in Ω , it is possible to define the following limit:

$$\delta(\Omega) = \lim_{n \rightarrow \infty} (m_n)^{1/n}, \quad (4.3)$$

which is the *transfinite diameter* of Ω [19]. Thus, one can say that the max norm of polynomials on Ω must grow asymptotically like $\delta(\Omega)^n$ as the degree n goes to ∞ .

Now let us consider the Lebesgue constant on Ω , and the associated Lebesgue points $\zeta_k \in \Omega$, which are the interpolation points where this minimal Lebesgue constant is attained: these are the best possible points to use as interpolation points in Ω , when one might have to interpolate any function whatsoever; that is, these are the best one can do without reference to the function being interpolated. It turns out that very little is known in general about Lebesgue points, though for certain domains and degrees they are known exactly.

An easier set of points to compute, given Ω , is the set of *Fekete points*, which are defined in terms of a domain Ω and a basis ϕ as the $n + 1$ points \mathbf{x}_F that maximize the generalized Vandermonde determinant $\det V$ where

$$\mathbf{V} = \begin{bmatrix} \phi_0(x_0) & \phi_1(x_0) & \cdots & \phi_{n+1}(x_0) \\ \phi_0(x_1) & \phi_1(x_1) & \cdots & \phi_{n+1}(x_1) \\ \vdots & & \ddots & \vdots \\ \phi_0(x_{n+1}) & \phi_1(x_{n+1}) & \cdots & \phi_{n+1}(x_{n+1}) \end{bmatrix}. \quad (4.4)$$

This is related to the question of small polynomials on Ω because any polynomial $p(z) = \sum_{k=0}^n c_k \phi_k(z)$ can be expressed via the Lagrange basis (for example in barycentric form) as a linear combination of values of $p(z)$ at the Fekete points \mathbf{x}_F , which are

$$\mathbf{p}(\mathbf{x}_F) = \mathbf{V}\mathbf{c} \quad (4.5)$$

and if $\|\mathbf{V}\|$ is large, then $|\mathbf{c}| \leq \|\mathbf{V}^{-1}\| \|\mathbf{p}(\mathbf{x}_F)\|$ has some chance to be small. In fact one wants to do more, to make sure that \mathbf{V} is *well-conditioned*, not just has a large determinant; and that is why Fekete points are good but not optimal.

However, one may show that in the limit as $n \rightarrow \infty$ the size of the operator norms one gets by interpolating at Fekete points approaches (from above, naturally) the asymptotic growth rate shown by the transfinite diameter (namely $\delta(\Omega)^n$).

Thus we see that Fekete points for the interpolation region under consideration, namely Ω , may prove to be good choices; however, research in the real two-dimensional case over simplexes such as triangles, and higher-dimensional simplexes, shows that Fekete points are not optimal, and that better points can be computed, for a given region [5].

For the first question, namely, for a given set of nodes \mathbf{x} , for what region Ω is $B(z)$ small, it seems intuitively clear that there is a region for which $B(z)$ is small indeed. For instance, if we take Ω to be the union of the $n + 1$ discs of fixed radius ε centred at each $x_k \in \mathbf{x}$, then the Lebesgue constant for \mathbf{x} in this (disconnected) region is $1 + K\varepsilon + O(\varepsilon^2)$, where $K = \max_k \sum_{j=0}^n |\phi'_j(x_k)|$. Since Lebesgue constants are always at least 1, this is nearly as good as one can do. In practice, we find that $B(z)$ is small for quite extensive regions near the given

interpolation points, though this is not yet well understood, as far as we know, and we hope to return to this in a future paper.

4.2. Pseudospectral plots

Consider an example. Take the matrix

$$\mathbf{T}^{-1} = \begin{bmatrix} 0 & 1 & 0 & -1 & 0 & 1 \\ 2 & 0 & 0 & 0 & 0 & 0 \\ 0 & 0 & 0 & 2 & 0 & -2 \\ -2 & 0 & 2 & 0 & 0 & 0 \\ 0 & 0 & 0 & 0 & 0 & 2 \\ 2 & 0 & -2 & 0 & 2 & 0 \end{bmatrix} \quad (4.6)$$

and form the essentially scalar matrix polynomial $\mathbf{P}(z) = (z\mathbf{T}^{-1})^7 - \mathbf{I}$. We sample this matrix polynomial at the eight nodes given by 0 and the 7th roots of unity. We then compute the contours of the pseudospectra by looking at the contours of $\|\mathbf{P}^{-1}(z)\|B(z)$. These are plotted in Figure 6.

The matrix \mathbf{T} has its eigenvalues the roots of the degree 6 Chebyshev polynomial, which are $\rho_k = \cos((2k+1)\pi/12)$, for $0 \leq k \leq 5$. Therefore the spectrum of this essentially scalar matrix polynomial are these Chebyshev roots multiplied by ω^j , for $0 \leq j \leq 6$, where ω is a primitive 7th root of unity.

For a discussion of the properties of essentially scalar matrix polynomials (which form good test problems for matrix polynomial eigenvalue problems), see [2].

In Figures 7 and 8 we show the effects of moving the nodes, leaving a ‘gap’ in one side. We clearly see the pseudospectral contours loosening.

4.3. Far from the nodes

We see that as $z \rightarrow \infty$, $B(z) = O(|z|^n)$. This conclusion only matters for a parameterized family of matrix polynomials that has a root z that goes to infinity as the parameter changes, *but whose values at the fixed nodes remain $O(1)$ as the parameter varies*. There is an example of such a family in [6] where it was shown that the condition number of such a root grows only like $O(|z|^2)$, because $B(z)/p'(z)$ grew this fast. Moreover, relative to the size of the root, the condition number is again reduced to $O(|z|)$. One wonders, at first, if reversing the nodes might help in this situation.

4.4. The effect of reversion

Consider the family of (scalar) polynomials used in [6]:

$$p(z) = C \left(\frac{z}{\rho} - r_1 \right) (z - r_2) \cdots (z - r_n) \quad (4.7)$$

and evaluate this polynomial on the fixed nodes x_0, x_1, \dots, x_n . This polynomial has a root at $r_1\rho$, and the absolute condition number of this root, namely $B(r_1\rho)/|p'(r_1\rho)|$ is $O(\rho^2)$ as ρ goes to infinity. Relative to $r_1\rho$, this is $O(\rho)$.

Reversing the polynomial, with $x_c^* = 0$ and $R = R^* = 1$, we get a new polynomial with a root at $1/(r_1\rho)$. The absolute condition number of this root is easily seen to be $O(1)$ as $\rho \rightarrow \infty$, a big improvement; however, relative to the root, it is $O(\rho)$ again.

It remains to be seen if reversion, which tightens the pseudospectra, will prove useful in computation. As in [9], reversion may be an essential practical step in numerical algorithms for GCD by values. This will be investigated in a future paper.

Now let us give examples of pseudospectra. Consider the circulant matrix polynomial

$$\mathbf{P}(z) = \begin{bmatrix} T_0(z) & T_1(z) & T_2(z) \\ T_2(z) & T_0(z) & T_1(z) \\ T_1(z) & T_2(z) & T_0(z) \end{bmatrix} \quad (4.8)$$

where $T_k(z)$ is the k th Chebyshev polynomial of the first kind. This is the case $n = 2$, $s = 3$ of a family of such matrices. The eigenvalues of this matrix are 0 , $-1/2$, $-3/4 \pm i\sqrt{3}/4$, and a double root at 1 .

Circulant matrices are all diagonalizable by the Fourier matrix [10], and hence the eigenvalues of circulant matrix polynomials are simply the roots of $\sum_{k=0}^{n-1} \omega^{jk} p_k(z)$, for $1 \leq j \leq n$ and ω is a primitive n th root of unity. Therefore, such matrix polynomials make simple test cases for polynomial eigenvalue software.

If we interpolate this particular degree 2 matrix polynomial at the 3rd roots of unity, and take that as our representation of $\mathbf{P}(z)$, then the pseudospectra of $\mathbf{P}(z)$ in this basis are plotted in Figure 9. Reversing this matrix polynomial (using $x_c = 0$ and $R = R^* = 1$) on these nodes gives us a matrix polynomial whose pseudospectra are plotted in Figure 10. Notice that the pseudospectral contours are much wider around the root at -2 in the reversed graph than they are around the corresponding root $-1/2$ in the original. However, in the original, the pseudospectra of $-1/2$ and 0 have merged by $\varepsilon = 10^{-1/2}$.

Now, consider some higher-degree circulant examples, in Figures 11 and 12. The figures show that the roots are not very sensitive to perturbation (one must take ε quite large to make the roots change), and show just which roots do merge to form clusters.

The final figure in the text, Figure 13, shows a graph of the contours of the Lebesgue function for interpolation at the 12 Chebyshev nodes on the interval $[-1, 1]$. The tighter contours at the endpoints show that zeros of polynomials near the endpoints are more likely to show sensitivity to perturbation, when the polynomials are expressed in terms of the Lagrange interpolants on these nodes.

5. Conclusions

We have shown in this paper that the pseudospectrum of matrix polynomials can depend very strongly on the basis used, and on the placement of the nodes in an interpolatory Lagrange basis. We have given new formulae for reversion of polynomials directly in Lagrange bases. We have given a geometric explanation of why surrounding a polynomial eigenvalue with nodes improves the conditioning (tightens the pseudospectra).

The arguments of this paper illuminate the Bernstein basis case, as well. If we examine the sum

$$B(z) = \sum_{k=0}^n |B_k^n(z; a, b)| \quad (5.1)$$

where each $B_k^n(z; a, b) = \binom{n}{k} (z-a)^k (b-z)^{n-k} / (b-a)^n$ is a Bernstein polynomial, and we have taken $\alpha_k = 1$ for all k , then because these polynomials are positive on $a < z < b$ and moreover sum to 1, we see that the amplification factor for the condition number is merely 1, which is as small as possible, everywhere across the interval. This is another way of showing that Bernstein bases are optimal in this sense. Investigation of the contours of $B(z)$ in the complex plane shows that they are ovals (perhaps ellipses) surrounding $[a, b]$, and their values grow slowly; near $\pm i$, however, the tops and bottoms of the unit circle, the values are large (much larger than that for the Lagrange basis using interpolation at roots of unity).

Another basis that is known to be good on an interval is interpolation at Chebyshev nodes ($\cos \pi(k+1/2)/n$, for $0 \leq k \leq n$). If we graph $B(x)$ on $-1 \leq x \leq 1$, we see that it oscillates, being 1 at the nodes, but never higher than a value that grows only slowly with the degree; in fact, this factor is less than or equal to $\frac{2}{\pi} \ln n + 1$, which bounds the Lebesgue constant for this set of nodes. See Figure 13 for the contours of the Lebesgue function for this set of nodes. This is to be contrasted with interpolation on uniform nodes, which have a Lebesgue constant that grows exponentially with n . A graph of $B(x)$ for only 12 uniform nodes needs to be plotted on a logarithmic scale!

The techniques of this paper show that this classical theory of Lebesgue functions and constants can be connected to the theory of pseudospectra of matrix polynomials, and gives insight into how one should choose interpolation nodes; contrariwise, the analysis of this paper shows that computation of polynomial eigenvalues of interpolated matrix polynomials can be reliable, namely when the nodes are close to and surround the polynomial eigenvalues.

Acknowledgements. We are grateful to Peter Lancaster for suggesting that we look at the reversal of a matrix polynomial in the Lagrange basis. Dhavide Aruliah was very helpful in discussions of this material. Finally, the referees pointed out several links to the vast literature on polynomial interpolation, and provided useful feedback to improve the paper.

References

- [1] Amirhossein Amiraslani. *Algorithms for Matrices, Polynomials, and Matrix Polynomials*. PhD thesis, University of Western Ontario, London, Canada, May 2006.
- [2] Amirhossein Amiraslani, Dhavide Aruliah, and Robert M. Corless. The Rayleigh quotient iteration for generalized companion matrix pencils. *submitted*, 2006.
- [3] Amirhossein Amiraslani, Robert M. Corless, and Peter Lancaster. Linearization of matrix polynomials expressed in polynomial bases. *submitted*, 2007.
- [4] Jean-Paul Berrut and Lloyd N. Trefethen. Barycentric Lagrange interpolation. *SIAM Review*, 46(3):501–517, 2004.
- [5] Qi Chen and Ivo Babuška. Approximate optimal points for polynomial interpolation of a real function in an interval and in a triangle. *Computer Methods in Applied Mechanics and Engineering*, 128:405–417, 1995.
- [6] Robert M. Corless. *Symbolic-Numeric Computation*, chapter On a generalized Companion Matrix Pencil for Matrix Polynomials Expressed in the Lagrange basis, page to appear. Birkhauser, 2006.
- [7] Robert M. Corless, Laureano Gonzalez-Vega, and Azar Shakoori. Geometric applications of the Bézout matrix in the Lagrange basis. *in preparation*, 2007.
- [8] Robert M. Corless and Stephen M. Watt. Bernstein bases are optimal, but, sometimes, Lagrange bases are better. In *Proceedings of SYNASC, Timisoara*, pages 141–153. MIRTON Press, September 2004.
- [9] Robert M. Corless, Stephen M. Watt, and Lihong Zhi. *QR* factoring to compute the GCD of univariate approximate polynomials. *IEEE Transactions on Signal Processing*, 2004.
- [10] Philip J. Davis. *Circulant Matrices*. Chelsea, 1994.
- [11] I. George Gohberg, P. Lancaster, and L. Rodman. *Matrix polynomials*. Academic Press, 1982.
- [12] Nicholas J. Higham. *Accuracy and Stability of Numerical Algorithms*. Society for Industrial and Applied Mathematics, Philadelphia, PA, USA, second edition, 2002.
- [13] Nicholas J. Higham. The numerical stability of barycentric Lagrange interpolation. *IMA Journal of Numerical Analysis*, 24:547–556, 2004.
- [14] Nicholas J. Higham, D. Steven Mackey, Niloufer Mackey, and Françoise Tisseur. Symmetric linearizations for matrix polynomials. *SIAM J. Matrix Anal. Appl.*, 29(1):143–159, 2006.
- [15] Nicholas J. Higham, D. Steven Mackey, and Françoise Tisseur. The conditioning of linearizations of matrix polynomials. *SIAM J. Matrix Anal. Appl.*, 28(4):1005–1028, 2006.
- [16] Peter Lancaster and Panayiotis Psarrakos. On the pseudospectra of matrix polynomials. *SIAM J. Matrix Anal. and Appl.*, 27:115–129, 2005.
- [17] Dinesh Manocha and James W. Demmel. Algorithms for intersecting parametric and algebraic curves II; multiple intersections. *Computer Vision, Graphics and Image Processing: Graphical Models and Image Processing*, 57(2):81–100, 1995.
- [18] Ivan Niven. *Maxima and Minima without Calculus*, volume 6 of *Dolciani Mathematical Expositions*. Mathematical Association of America, 1981.

- [19] T. Rivlin. *Chebyshev polynomials: from approximation theory to number theory*. Wiley, 1990.
- [20] Françoise Tisseur. Backward error and condition of polynomial eigenvalue problems. *Linear Algebra and its Applications*, 309:339–361, 2000.
- [21] Françoise Tisseur and Nicholas J. Higham. Structured pseudospectra for polynomial eigenvalue problems, with applications. *SIAM J. Matrix Anal. Appl.*, 23(1):187–208, 2001.

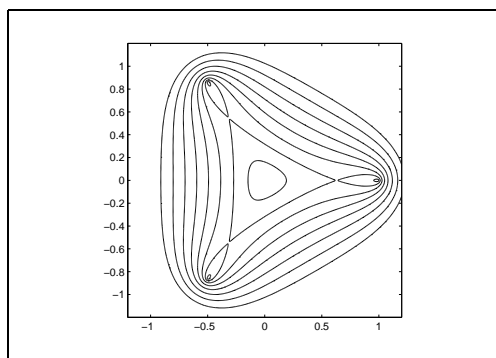


FIGURE 1. Contours of $B(z)$ where the nodes are at the 3 cube roots of unity. The contours are $[1, r^{1/4}, r, r^{9/4}, r^{16/4}, \dots]$ where $r = B(r_m) \approx 1.029$ is the unique maximum value of $B(z)$ on $0 \leq z \leq 1$. The contour that crosses itself has this maximum height, in this case about 3% greater than the minimum possible value. We see greater than geometric increase in $B(z)$ outside the triangular region bounded by the nodes.

Robert M. Corless
 Dept. Applied Mathematics
 University of Western Ontario
 London, CANADA
 e-mail: rcorless@uwo.ca

Nargol Rezvani
 Dept. Computer Science
 University of Toronto
 Toronto, CANADA
 e-mail: nrezvani@cs.utoronto.edu

Amirhossein Amiraslani
 Dept. Mathematics & Statistics
 University of Calgary
 Calgary, CANADA
 e-mail: amiram@math.ucalgary.ca

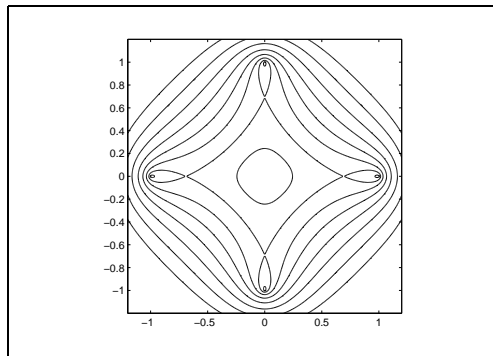


FIGURE 2. Contours of $B(z)$ where the nodes are at the 4 fourth roots of unity. The contours are $[1, r^{1/4}, r, \dots]$ and thereafter grow like r^{k^2} , where $r = B(r_m) = (10 + 7\sqrt{7})/27 \approx 1.0563$ is the unique maximum value of $B(z)$ on $0 \leq z \leq 1$. The contour that crosses itself has this maximum height, in this case about 6% greater than the minimum possible value. Again, we see greater than geometric increase in $B(z)$ outside the square diamond region bounded by the nodes.

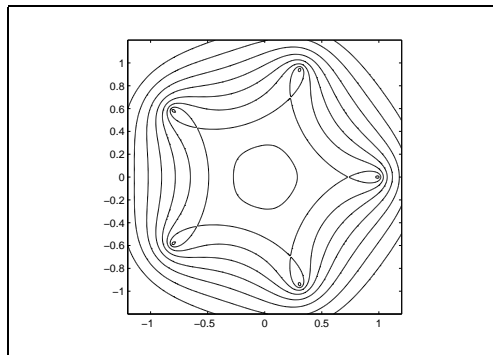


FIGURE 3. Contours of $B(z)$ where the nodes are at the fifth roots of unity. The contours are $[1, r^{1/4}, r, \dots]$ and thereafter grow like r^{k^2} , where $r = B(r_m) \approx 1.0845$ is the unique maximum value of $B(z)$ on $0 \leq z \leq 1$. The contour that crosses itself has this maximum height, in this case about 8% greater than the minimum possible value. We see greater than geometric increase in $B(z)$ outside the pentagonal region bounded by the nodes.

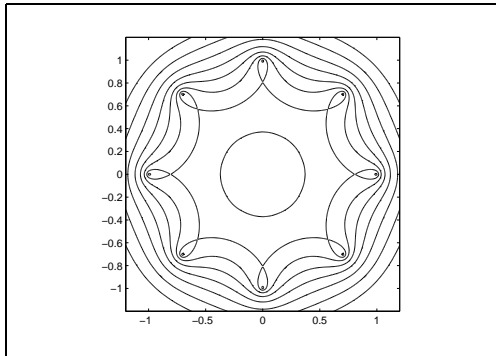


FIGURE 4. Contours of $B(z)$ where the nodes are at the eighth roots of unity. The contours are $[1, r^{1/4}, r, \dots]$ and thereafter grow like r^{k^2} , where $r = B(r_m) \approx 1.157$ is the unique maximum value of $B(z)$ on $0 \leq z \leq 1$. The contour that crosses itself has this maximum height, in this case about 16% greater than the minimum possible value. We see greater than geometric increase in $B(z)$ outside the octagonal region bounded by the nodes.

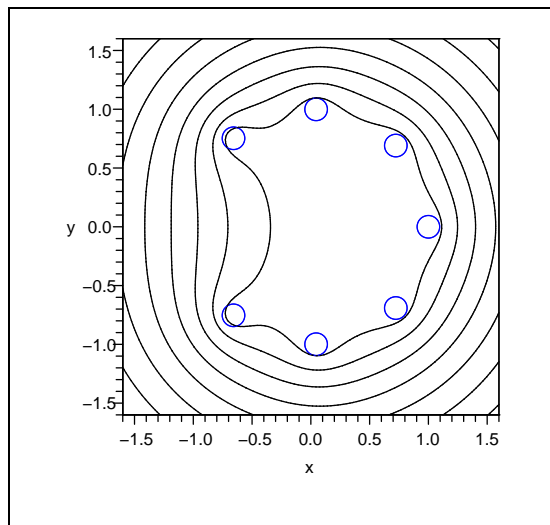


FIGURE 5. Contours of $B(z)$ where the nodes are no longer symmetric. As we see, the disturbance of the symmetry makes an alteration in the contours, but the overall picture remains similar. In this case the contours are at 1, 2, 4, \dots

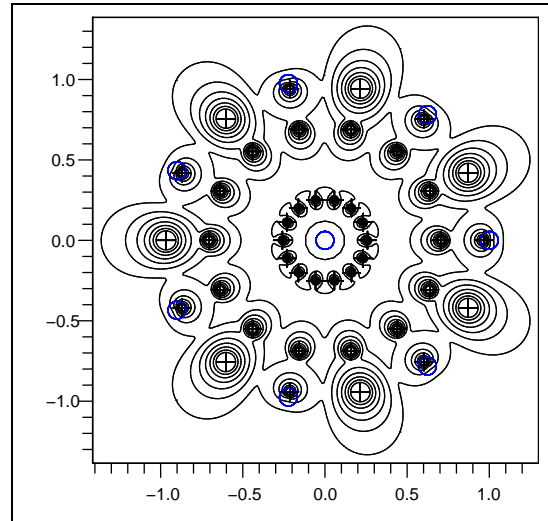


FIGURE 6. The pseudospectrum of an essentially scalar matrix polynomial. The symmetry of the node placement with respect to the polynomial eigenvalues ensures ‘tight’ pseudospectral contours. Eigenvalues are shown with +.

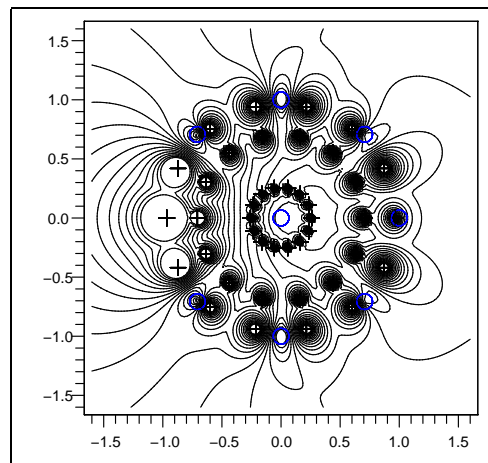


FIGURE 7. The pseudospectrum of an essentially scalar matrix polynomial. The asymmetry of the node placement (the nodes are the eighth roots of unity, except -1 , and with 0 additionally) with respect to the polynomial eigenvalues, compared with Figure 6, shows a ‘loosening’ of pseudospectral contours away from the nodes.

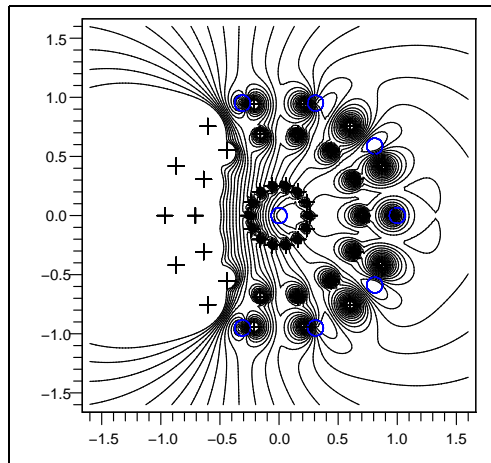


FIGURE 8. The pseudospectrum of an essentially scalar matrix polynomial. The further asymmetry of the node placement with respect to the polynomial eigenvalues (the gap at -1 is further spread than in previous figures), compared with Figures 6 and 7 shows still greater ‘loosening’ of pseudospectral contours away from the nodes.

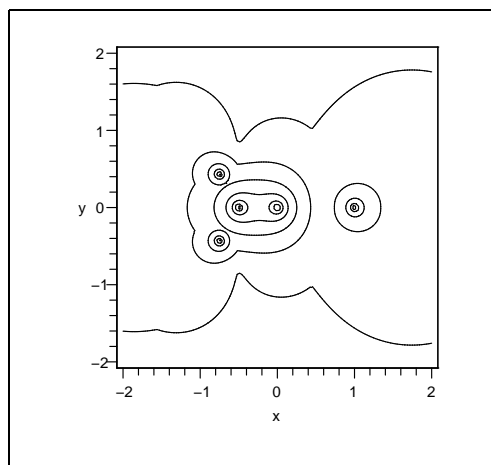


FIGURE 9. The pseudospectrum of a circulant matrix polynomial. The six finite polynomial eigenvalues are 0 , $-1/2$, $-3/4 \pm i\sqrt{3}/4$, and a double root at 1 . The contours are at 10^{-3} , $10^{-2.5}$, 10^{-2} , $10^{-1.5}$, 10^{-1} , $10^{-0.5}$, and 1 . Not all contours are visible.

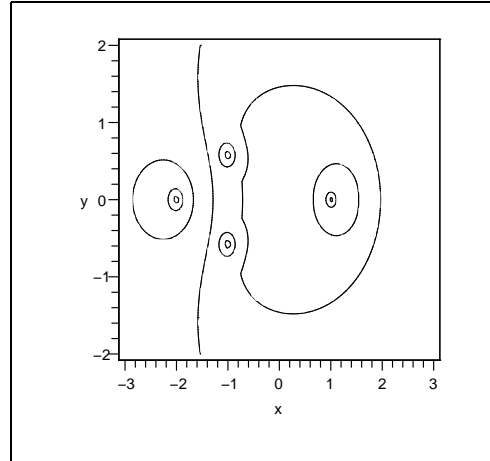


FIGURE 10. The pseudospectrum of a reversed circulant matrix polynomial. The finite polynomial eigenvalues are -2 , $-1 \pm i\sqrt{3}/3$, a double root at 1 . There is one root at infinity. The contours are at 10^{-3} , $10^{-2.5}$, 10^{-2} , $10^{-1.5}$, 10^{-1} , $10^{-0.5}$, and 1 . Not all contours are visible.

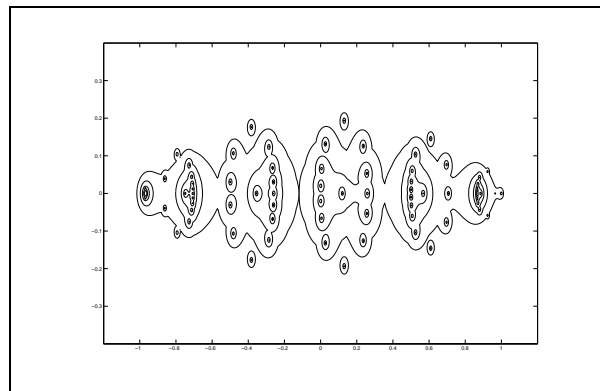


FIGURE 11. The pseudospectrum of a degree 12, 13×13 circulant matrix polynomial with entries $T_j(z)$ (j th Chebyshev polynomials). We interpolate this at the 13th roots of unity. The contours are at 10^{-3} , $10^{-2.5}$, 10^{-2} , $10^{-1.5}$, 10^{-1} , $10^{-0.5}$, and 1 . Not all contours are visible.

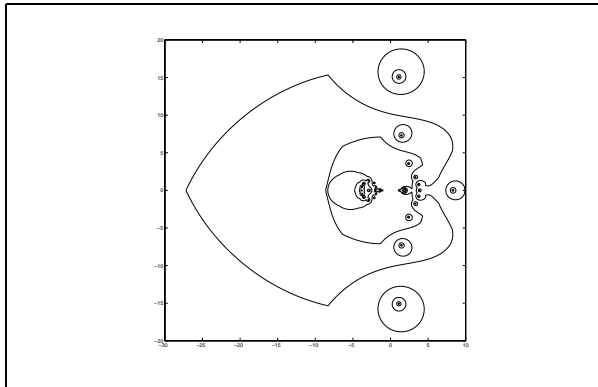


FIGURE 12. The reversed pseudospectrum of a degree 12, 13×13 circulant matrix polynomial with entries $T_j(z)$ (j th Chebyshev polynomials), again interpolated at the 13th roots of unity. The contours are at 10^{-3} , $10^{-2.5}$, 10^{-2} , $10^{-1.5}$, 10^{-1} , $10^{-0.5}$, and 1. Not all contours are visible, and indeed some of the larger polynomial eigenvalues are not shown.

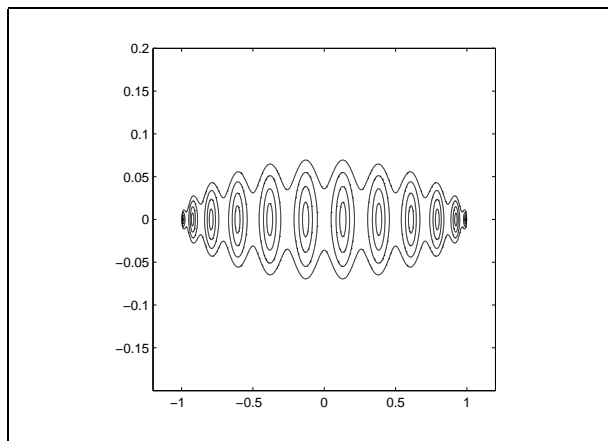


FIGURE 13. Interpolation at 12 Chebyshev nodes produces a Lebesgue function which has the contours shown in this figure (the contours are equally spaced between 1 and 2.25). Pseudospectra would be spread by the factors represented by the values shown above. This graph is in accordance with the classical results on the Lebesgue constants for the Chebyshev points [19].